

Article

Numerical Studies on the Action Mechanism of Combustion Intermediates and Free Radicals on Nitrogen Oxides under Oil-Water Blended Conditions

Xiumin Yu ^{1,2}, Fengshuo He ^{1,2} , Yaodong Du ^{1,2,*} and Zezhou Guo ^{1,2}

¹ State Key Laboratory of Automotive Simulation and Control, Jilin University, Changchun 130022, China; yuxm@jlu.edu.cn (X.Y.); hefengshuo2004@sina.com (F.H.); zezhouguo@126.com (Z.G.)

² College of Automotive Engineering, Jilin University, Changchun 130022, China

* Correspondence: duyud@jlu.edu.cn; Tel./Fax: +86-0431-8516-7419

Received: 5 March 2018; Accepted: 21 March 2018; Published: 23 March 2018



Featured Application: Clean combustion technology of internal combustion engine and internal purification for combustion reactor.

Abstract: The action mechanism of combustion intermediates and free radicals on nitrogen oxides have been evaluated. Based on chemical reaction dynamics and modern statistical theory, the subject was investigated by means of numerical simulation. A wide water/oil ratio and a wide air/fuel ratio were also taken into account. Some main conclusions were drawn that the reaction response of H₂O₂ is lagged behind, with the increase of water mass fraction from 10% to 30%. The maximum generation rate is 2.77%, 5.67%, 8.38% and the maximum consumption rate is 3.55%, 6.80%, 13.01% lower than that without water. Water addition leads to decline of the maximum generation rate of NO, N₂O, NO₂ by 15.24%, 9.21%, 14.78% on average. Further, the saliency factor is explored in the main reaction process depending on the correlation analysis and the sensitivity analysis method. According to the degree of the significance, OH > O > H₂ for NO, O > H₂ > OH > HO₂ for N₂O, and OH > H₂ > O > H₂O₂ > HO₂ for NO₂. In the case of oil-water blended, H + O₂ ⇌ O + OH and H₂O₂(+M) ⇌ 2OH(+M) promote the generation of OH and O at the beginning of the second stage, but H + O₂(+M) ⇌ HO₂(+M), HO₂ + OH ⇌ H₂O + O₂, H₂O₂ + OH ⇌ H₂O + HO₂ play an inhibitory role in the generation of OH and O.

Keywords: chemical reaction dynamics; oil-water blended; nitrogen oxides; Spearman rank correlation; sensitivity analysis

1. Introduction

At present, the problem of environmental pollution has attracted more and more attention, especially the problem of nitrogen oxide pollution, which has perplexed us for a long time. The generation of NO_x is divided into thermal NO_x, fast NO_x and fuel NO_x. Thermal NO_x refers to nitrogen oxides produced by oxidation of N₂ in the air at high temperature. The generation mechanism of the fast NO_x is that a large amount of NO_x is produced rapidly in the surface of the flame when the excess air coefficient is less than 1. The generation of fuel NO_x depends on the nitrogen compounds in the fuel. Previous studies have demonstrated that the components of nitrogen oxides emission produced during the combustion process are mainly NO, and a small amount of NO₂, N₂O and so on. But NO will be reoxidized to NO₂ in the air. In the control technologies of reducing nitrogen oxides emission, combustion with moderate water addition is an effective way [1,2].

Oil water emulsion and water injection are two common measures to introduce water into the combustion reaction, which is also regarded as the fuel improvement techniques. Elsanusi et al. [3]

performed a set of engine experiments at the condition of three engine speeds (1000, 2100 and 3000 rpm), three engine loads (20%, 50% and 80%), and three different levels of water concentration (5%, 10% and 15%). They concluded that the nitrogen oxides (NO_x) were significantly reduced with the increase of water content in the emulsion compared to their bases. One advantage of water injection when compared with EGR is the possible reduction of NO_x emissions either at low engine loads and high engine loads without a substantial increase in PM emissions [4].

Kokkulunk et al. [5] investigated the performance and efficiency of a diesel engine with a steam injection system by means of experiment and simulation. They come to conclusion that the steam injection had a positive effect on performance and NO emissions at all speed and didn't affect CO, CO_2 , HC emissions considerably. Tesfa et al. [6] conducted an engine experiment operated with biodiesel directly injected in the cylinder and water injected in the manifold. Some conclusion was got that when the water injection rate was 3 kg/h, NO_x was reduced by about 50% and this measure didn't result in significant changes in fuel consumption. In addition, the water injection in the intake manifold had little effect on the cylinder pressure and the heat release rate [7]. Kyriakides et al. [8] performed an experimental study with gasoline-ethanol-water ternary mixtures. They pointed out that the Otto engine requires no modifications to burn E40 and E40h (10% hydrous) efficiently with advantage of NO_x emissions reduction. Nag Jung Choi et al. [9,10] proposed that the combustion temperature of fuel is the most important factor that directly affecting the NO_x emissions from the engine. For biodiesel, the NO_x emission increases a little with increasing of biodiesel blend ratio in diesel engines fueled with biodiesel blend fuel. This could attribute to that the combustion chamber temperature of biodiesel is higher than that of diesel fuel. Because biodiesel is an oxygenated fuel.

All the references mentioned above are focused on the generation quantity of NO_x , which remained at the macro and phenomenal levels. Researchers are more inclined to explain the phenomenon that water addition into the combustion chamber can inhibit the generation of nitrogen oxides based on the physical property of water. Apparently, the latent heat of vaporization of water is high (40.8 kJ/mole at 100 °C, 1 atm), after introducing water into the combustion chamber, the adiabatic flame temperature reduces due to water vaporization. And it is generally believed that the generation conditions of NO_x are high temperature and oxygen enrichment. This explanation is reasonable, but not enough. Correspondingly, at the micro level, there are few studies focused on the chemical effects of water involved in the progress of NO_x reduction. Namely, the related mechanism is not clear. Some experimental studies have shown that small molecules and free radicals in the period of combustion have some influence on the generation of NO_x [11–13]. However, at present, most laboratories have no quantitative measurement of free radicals. Even in reference 13, planar-laser-induced fluorescence (PLIF) is used to measure the distribution of OH radical. By using planar-laser-induced fluorescence (PLIF) and laser-induced fluorescence (LIF) spectroscopy, the energy decay of incident light and fluorescence quenching will be the biggest barrier. It has a bad impact on the quantitative calibration and has a strict requirement for the output wavelength of the laser [14,15]. Experimental measurements have limitations, and therefore, numerical calculation is an alternative method.

In further microscopic research on emission problems, it is especially important for multi-level reaction analysis of reaction rate, concentration and reaction time of reaction products in chemical reaction kinetics. Hence, correlation analysis and sensitivity analysis are introduced. Correlation analysis is helpful for researchers to understand the generation and consumption process of combustion pollutants and free radicals in essence, so as to provide a theoretical basis and technical approach for effective control generation of nitrogen oxides. It is of innovative significance to study the process of NO_x generation at the condition of oil-water blended with the two means above. And the coupling of correlation analysis and sensitivity analysis can greatly improve the researchers' insight into the importance of each reaction way, thus realizing the purpose of controlling combustion [16]. Under different initial conditions and boundary circumstances, the efficiency of solving the governing equation is too low. The more parameters involved in the model, the more prominent the problem

is. Therefore, the introduction of correlation analysis and sensitivity analysis into the kinetics of elemental reaction has enriched the research means to make it possible to analyze the process of combustion [17]. The application of the coupling analysis to the generation of combustion pollutants is of great significance for analyzing the characteristics of pollutant generation, simplifying the reaction model and determining the suppression method.

In the present study, based on such realistic conditions, numerical methods enter into consideration. The valid mechanism analysis of combustion reaction process with oil-water-blended is focused. Based on correlation analysis and sensitivity analysis, the key intermediate products to control the yield of NO_x in oil-water-blended condition are obtained, and the main paths are analyzed as well.

2. Experimental Method and Experimental Setup

2.1. Experimental Method

For the numerical calculation of chemical reaction dynamics, CHEMKIN [18] is a common tool, which is suitable for analyzing the chemical reaction process. Its main function is to solve a series of chemical problems involved in combustion through the analysis and calculation of the chemical reaction mechanism. Because the software package has the characteristics of reasonable structure, good reliability and easy to transplant, it has become the mainstream calculation software in the field of combustion chemistry dynamics. Some thermodynamic data are provided in the form of the NASA chemical equilibrium code, which are showed as the following Equations (1)–(6) [19]. Seven coefficients ($a_{1k} \sim a_{7k}$) are given in a database file (e.g., therm.dat), which is provided by the mechanism file.

$$\frac{C_{pk}^0}{R} = a_{1k} + a_{2k}T_k + a_{3k}T_k^2 + a_{4k}T_k^3 + a_{5k}T_k^4 \quad (1)$$

$$\frac{H_k^0}{RT_k} = a_{1k} + \frac{a_{2k}}{2}T_k + \frac{a_{3k}}{3}T_k^2 + \frac{a_{4k}}{4}T_k^3 + \frac{a_{5k}}{5}T_k^4 + \frac{a_{6k}}{T_k} \quad (2)$$

$$\frac{S_k^0}{R} = a_{1k} \ln T_k + a_{2k}T_k + \frac{a_{3k}}{2}T_k^2 + \frac{a_{4k}}{3}T_k^3 + \frac{a_{5k}}{4}T_k^4 + a_{7k} \quad (3)$$

$$C_{vk}^0 = C_{pk}^0 - R \quad (4)$$

$$U_k^0 = H_k^0 - RT_k \quad (5)$$

$$G_k^0 = H_k^0 - T_k S_k^0 \quad (6)$$

The chemical reaction mechanism used in this paper comes from two parts. Chen et al. [20] developed a reduced mechanism, which contains 207 species and 1026 steps. The mechanism is based on five components ($\text{C}_6\text{H}_5\text{CH}_3$, iC_5H_{12} , iC_8H_{18} , nC_5H_{12} , nC_7H_{16}) gasoline surrogate mechanism, which comes from Lawrence Livermore National Laboratory (LLNL) [21]. This 207-species skeletal mechanism is validated under a wide range of conditions compared to the rapid compression machine (RCM) experimental data, and it has also been mentioned or verified widely in other research [22–24]. The mixture oil in this mechanism has similar properties to local oil products in Changchun, China, so the mechanism is suitable for this study and for future research.

The NO_x mechanism comes from GRI mech3.0 [25], which has been widely verified by experiments [26–28]. In order to study the effect of gasoline-water blended on NO_x , this work combines the NO_x mechanism in GRI mech3.0 and Chen mechanism to fulfill the research. And the composite mechanism is provided with Supplementary materials.

2.2. Experimental Setup

The research is carried out in a closed homogeneous batch reactor provided by CHEMKIN code [18]. This is a ‘Closed 0-D Reactor’, which is used to simulate constant volume combustion problems and solve the energy equation. Before running the project, some of the computing conditions need to be set up. For example, import the composite mechanism file in ‘Pre-Processing’ section and then set the solver properties. In this project, the absolute tolerance is set to 1.0×10^{-20} ; the relative tolerance is set to 1.0×10^{-8} ; the sensitivity absolute tolerance is set to 1.0×10^{-4} ; and the sensitivity relative tolerance is set to 1.0×10^{-4} . For quantitative analysis, the water-oil mass ratio (WOMR) is defined in Equation (7). The other properties of the oil and the experimental condition are presented in Table 1.

$$r = \frac{m_{\text{water}}}{m_{\text{oil}}} \times 100\% \quad (7)$$

Table 1. Properties of the oil and experimental settings.

Category	Value
Fuel mixture (mol. %)	C ₆ H ₅ CH ₃ : 37%, iC ₅ H ₁₂ : 27%, iC ₈ H ₁₈ : 27%, nC ₅ H ₁₂ : 5%, nC ₇ H ₁₆ : 4%
Dynamic viscosity (kg·m ⁻¹ ·s ⁻¹)	3.1×10^{-4} (at 25 °C, 1 atm) [29,30]
Density (kg·m ⁻³)	804 (at 25 °C, 1 atm) [29,30]
RON	95.4 [30,31]
MON	87.8 [30,32]
Oxidizer mixture (mol. %)	O ₂ : 21%, N ₂ : 78%, Ar: 1%
Initial condition	T: 800 K, P: 8 atm, V: 65 cm ³
λ	0.6, 0.8, 1, 1.2, 1.4
Water-oil mass ratio	0, 10%, 20%, 30%

3. Results and Discussion

3.1. Two Stages Reaction Processes

Figure 1a–c are at different coordinating scales. In Figure 1a, the reaction is divided into two stages. The first stage occurs after about 1.3 ms. For the phase of low temperature oxidation, the reaction of mixed gas is exothermic, and the temperature increases from 800 K to 1000 K. H₂O₂ and HO₂ are mainly produced at this stage and are considered as indicator products for the two-stage reaction. Decomposition of H₂O₂, H₂O₂ + M ⇌ 2OH + M (#16 elementary reaction in Chen mechanism plus GRI mech3.0) happens at 6.9 ms. For the combustion reaction, the large amount of OH generation marks the start of the burning. The three-body reaction H + O₂ + M ⇌ HO₂ + M (#9 elementary reaction in Chen mechanism plus GRI mech3.0) is an important radical recombination step, plays an important role as a chain terminating process at the second explosion limit and leads to relatively long induction times at conditions near the second limit [33]. The paramount condition that the system can enter the high temperature stage after the low temperature stage is that the low temperature reaction must be able to release enough heat to increase the temperature of the system. When the temperature reaches to 1000 K, the temperature rises sharply, and the mixture enters the high temperature oxidation stage. The high temperature reaction process releases a lot of heat, which provides the conditions for NO_x generation.

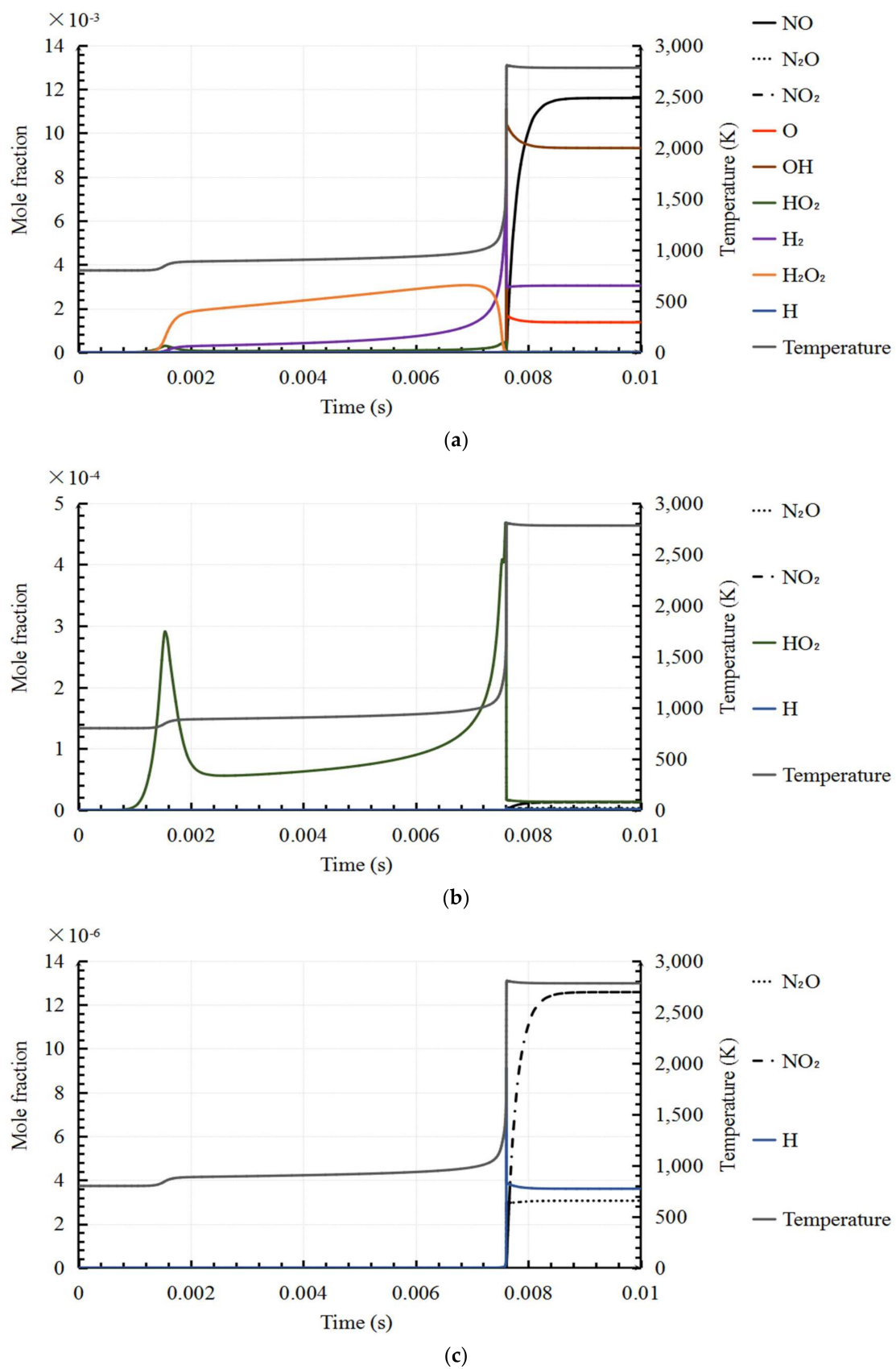


Figure 1. The iterative process of the intermediate products, NO_x and temperature ($\lambda = 1$, $\text{WOMR} = 0$). (a) Global comparison; (b) Detail comparison 1; (c) Detail comparison 2.

3.2. Intermediate Reaction Products (Small Molecules and Free Radicals) at Different WOMR

In Figure 2a, the variation of the reaction rate of H_2O_2 with different water/oil mass ratio is exhibited. Combined with Figures 1a and 2b,c, the generation of H_2O_2 occurred between 0.001 s and 0.002 s and the consumption occurred between 0.007 s and 0.008 s. When the water mass fraction increases from 10% to 30%, the response of the reaction of H_2O_2 is lagged behind, and the maximum generation rate is 2.77%, 5.67%, 8.38% lower than that without water, and the maximum consumption rate is 3.55%, 6.80%, 13.01% lower than that without water. It shows that both reaction delay and peak value decrease cause the increase of heat needed for activation reaction at the same activation energy and reaction temperature when water is introduced to inhibit the chain reaction. The existence of water plays a role in controlling the rate of the main element reaction.

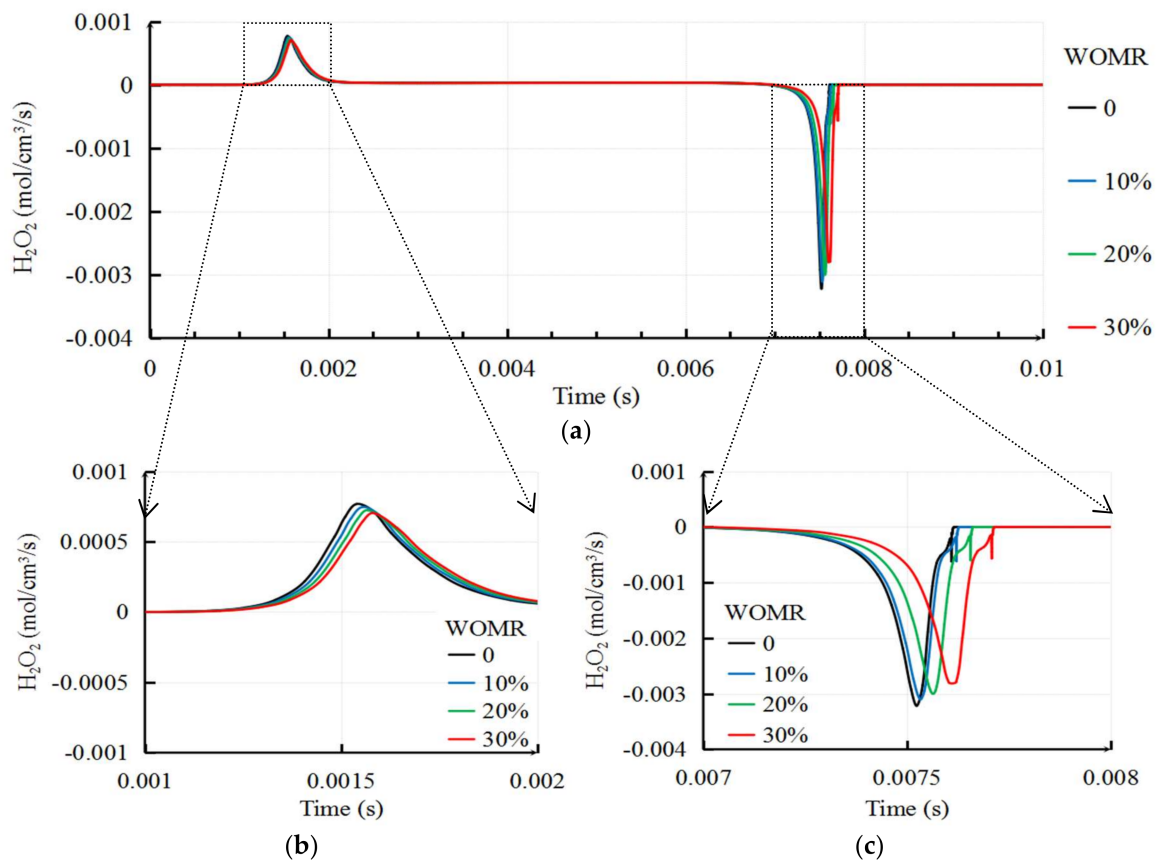


Figure 2. Reaction rate of H_2O_2 at different WOMR ($\lambda = 1$). (a) Global profile comparison; (b) Detail profile comparison 1; (c) Detail profile comparison 2.

Figure 3 shows the reaction rate of H_2 at different WOMR. Hydrogen has the advantages of low ignition energy, high flame propagation speed, high diffusion rate and wide ignition limit [34–36]. Therefore, hydrogen addition can effectively increase combustion stability. The primary hydrogen production reaction in this mechanism is: $\text{NH} + \text{H}_2\text{O} \rightleftharpoons \text{HNO} + \text{H}_2$ (#1032 elementary reaction in Chen mechanism plus GRI mech3.0), in which the positive reaction requires very high activation energy, $E_a = 13.850$ kJ/mol. With the increase of water, the temperature of the system decreases and the generation rate of H_2 decreases significantly, and the reaction is pushed back. But another elementary reaction $\text{NH} + \text{NO} \rightleftharpoons \text{N}_2 + \text{OH}$ (#1033 elementary reaction in Chen mechanism plus GRI mech3.0) mainly occurs in the reductive environment. So under this circumstance, the above two steps will result in a scramble for the NH radical. Then the final result of the effect is that the NH is oxidized by excessive H_2O , so the reduction process of NO is hindered, resulting in a slight increase of the yield of NO .

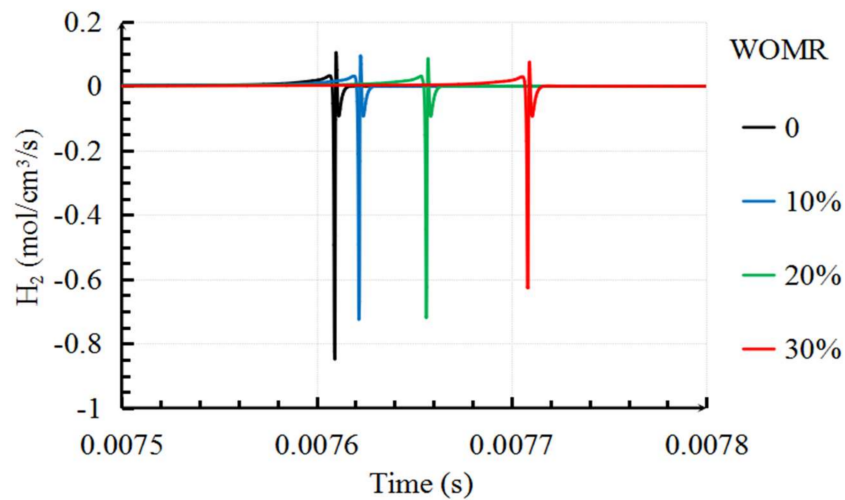


Figure 3. Reaction rate of H_2 at different WOMR ($\lambda = 1$).

From Figure 4, it can be seen that with the increase of water content, the reaction rates of OH, HO_2 , H and O decrease in varying degrees and are accompanied by the back shift of the peak value. At the same time, there is also the transfer process of material and energy between the four intermediate products. These reactions occur at the high temperature stage at the end of the first stage. Because of the high temperature, the intense reaction, the short reaction time, and the competition for the same components, there is a relationship between these reactions, forming a closed loop, as shown in Table 2. In a moment, the concentration of OH and O increases sharply, which causes the generation of many active centers. Ultimately, the activation center concentration is the key factor affecting the combustion of the fuel. This is the starting point of the second stage combustion. The concentration of OH and O decreases after some chain carrier is destroyed. Then the system reaches the steady state gradually.

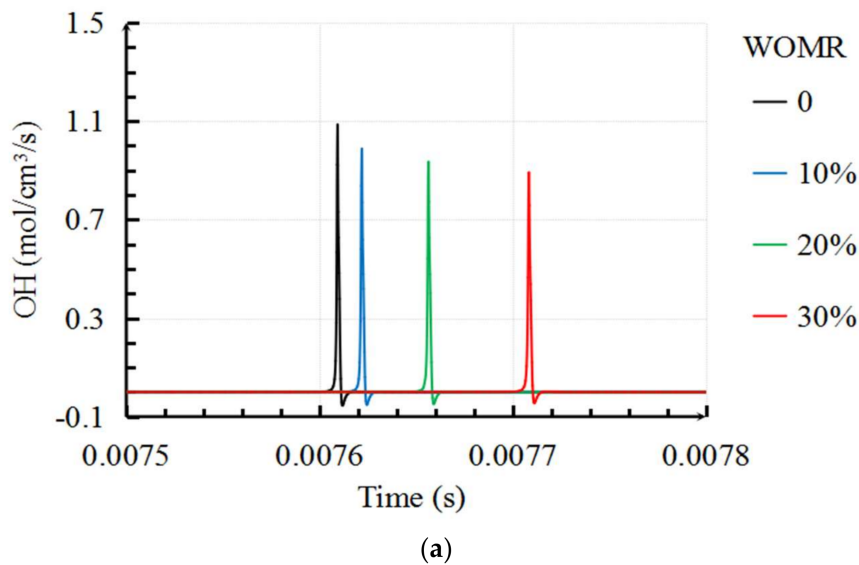
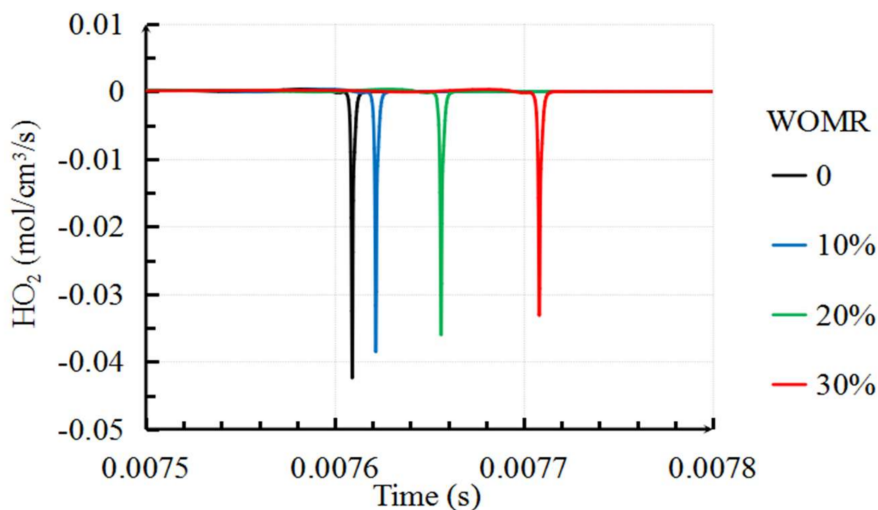
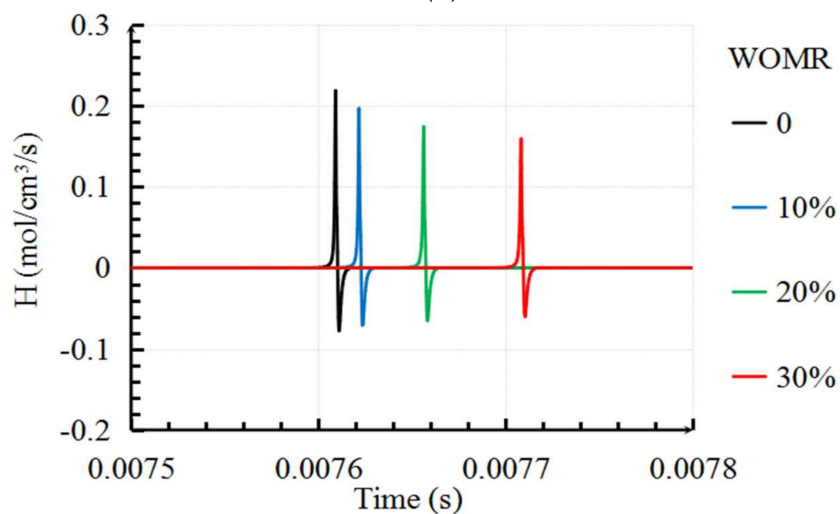


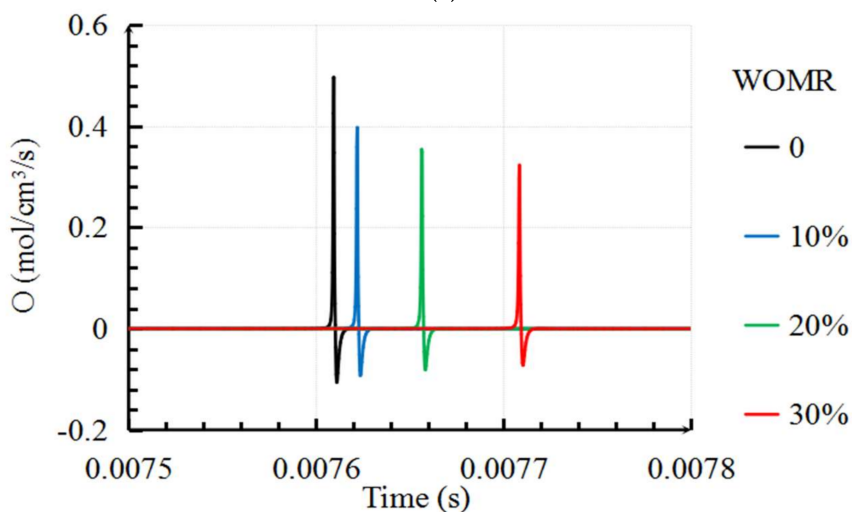
Figure 4. Cont.



(b)



(c)



(d)

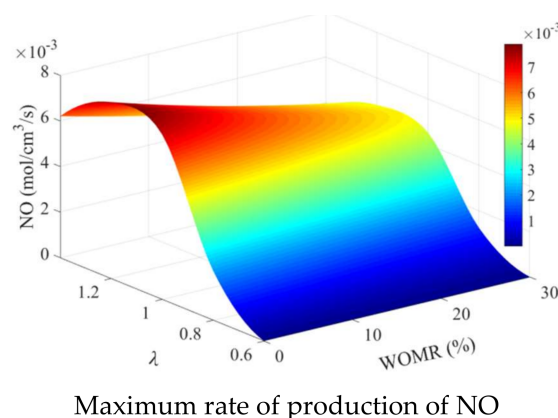
Figure 4. Reaction rate of OH, HO₂, H and O at different WOMR ($\lambda = 1$). (a) Reaction rate of OH; (b) Reaction rate of HO₂; (c) Reaction rate of H; (d) Reaction rate of O.

Table 2. Elementary reactions sequence in recombination mechanism.

Reaction	Serial Number
$\text{H} + \text{O}_2 \rightleftharpoons \text{O} + \text{OH}$	1
$\text{O} + \text{H}_2 \rightleftharpoons \text{H} + \text{OH}$	2
$\text{OH} + \text{H}_2 \rightleftharpoons \text{H} + \text{H}_2\text{O}$	3
$\text{O} + \text{H}_2\text{O} \rightleftharpoons 2\text{OH}$	4
$\text{H}_2\text{O} + \text{M} \rightleftharpoons \text{H} + \text{OH} + \text{M}$	8
$\text{H} + \text{O}_2(+\text{M}) \rightleftharpoons \text{HO}_2(+\text{M})$	9
$\text{HO}_2 + \text{H} \rightleftharpoons \text{H}_2 + \text{O}_2$	10
$\text{HO}_2 + \text{OH} \rightleftharpoons \text{H}_2\text{O} + \text{O}_2$	13
$\text{H}_2\text{O}_2(+\text{M}) \rightleftharpoons 2\text{OH}(+\text{M})$	16
$\text{H}_2\text{O}_2 + \text{H} \rightleftharpoons \text{H}_2 + \text{HO}_2$	18
$\text{H}_2\text{O}_2 + \text{O} \rightleftharpoons \text{OH} + \text{HO}_2$	19
$\text{H}_2\text{O}_2 + \text{OH} \rightleftharpoons \text{H}_2\text{O} + \text{HO}_2$	20

3.3. Coupling Analysis at Water Mixing and Variable Excess Air Coefficient Conditions

Figure 5 shows the mole fraction map of free radicals corresponding to maximum rate map of production of NO, Figure 6 shows the mole fraction map of free radicals corresponding to maximum rate map of production of N₂O, and Figure 7 shows the mole fraction map of free radicals corresponding to maximum rate map of production of NO₂. Because the corresponding time of the maximum production rate of NO, N₂O, and NO₂ is very close to each other, free radicals have little change in the maps of the three groups. In these three groups of figures, because the temperature reduces obviously, the starting point of the high temperature oxidation stage is delayed, the duration of the high temperature is shorter and the generation rate of NO_x decreases, with the increase of the proportion of water in the fuel. When the water content increases by 10%, the maximum NO generation rate decreases by 15.24% on average, the maximum N₂O generation rate decreases by 9.21% on average, and the maximum NO₂ generation rate decreases by 14.78% on average. In the distribution of free radicals mole fraction, H, HO₂ and H₂O₂ show obviously non monotonicity in lambda direction, which is inconsistent with the monotonicity of NO_x generating rate map. It can be roughly estimated that the above three free radicals are not very closely related to NO_x generation. For O and OH, the mole concentration map can be observed clearly, which is consistent with the NO_x generation rate in the two-dimensional space of lambda and WOMR, in the three groups of figures. In order to further explore, the results of the above maps will be analyzed by correlation analysis and sensitivity analysis.

**Figure 5.** Cont.

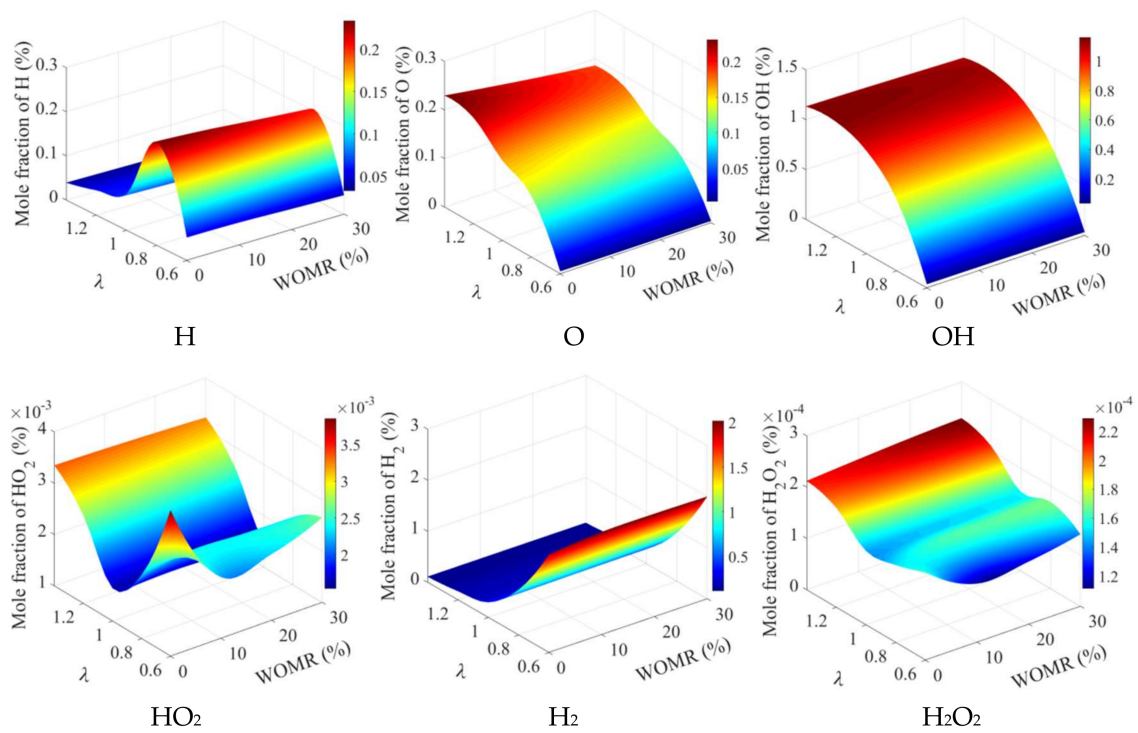


Figure 5. Mole fraction of free radicals corresponding to maximum rate of production of NO.

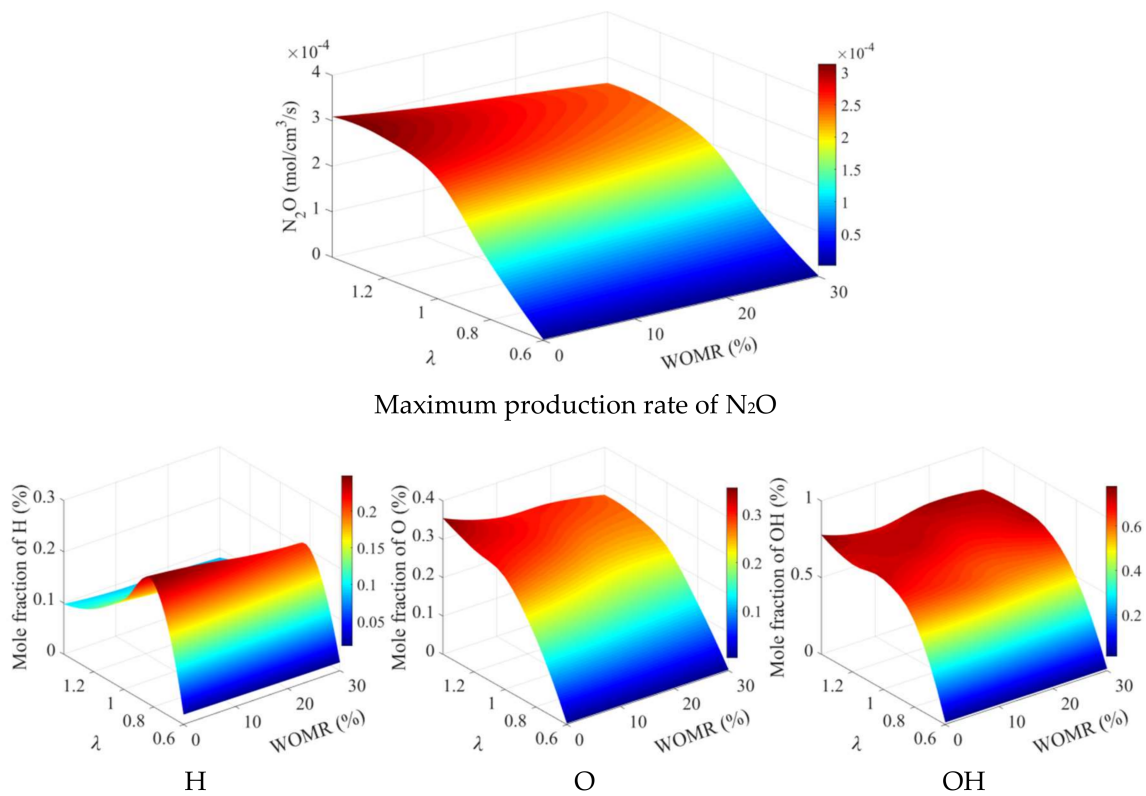


Figure 6. Cont.

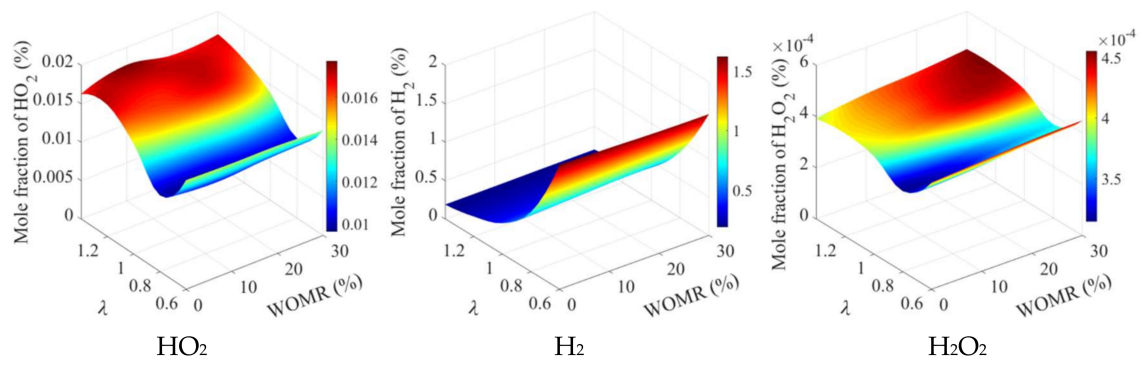
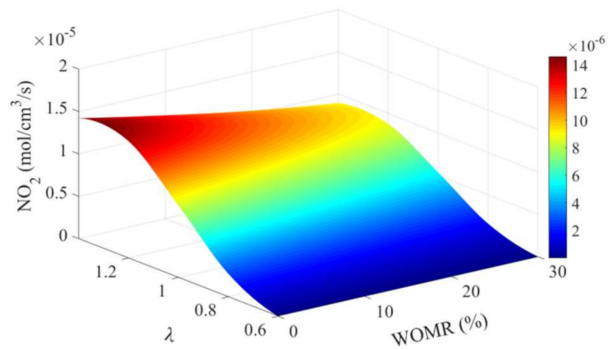


Figure 6. Mole fraction of free radicals corresponding to maximum rate of production of N₂O.



Maximum production rate of NO₂

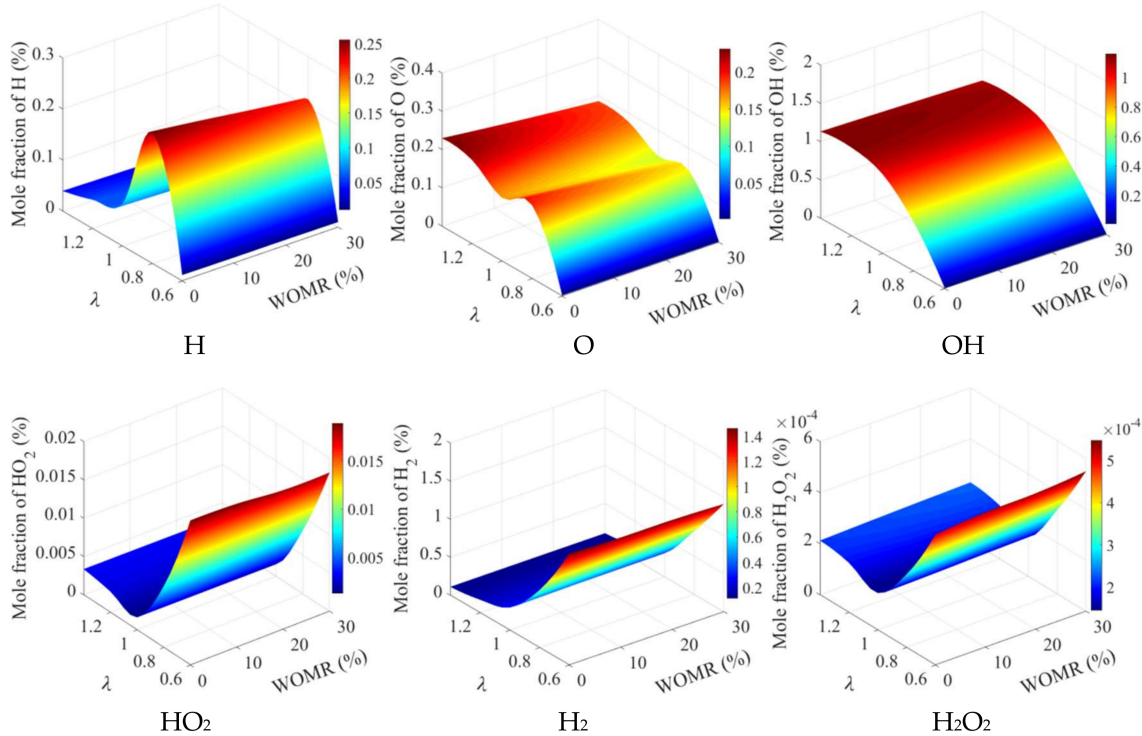


Figure 7. Mole fraction of free radicals corresponding to maximum rate of production of NO₂.

3.3.1. Correlation Analysis

In order to further explain the relative relationship between the small molecules of the free radicals and the NO_x, the correlation coefficient algorithm is introduced to illustrate this problem.

Number of pairs, such as (x₁, y₁), (x₂, y₂), . . . , (x_n, y_n) are given. It is necessary to check whether the two variables, X and Y, are related. The traditional Pearson product-moment correlation coefficient (PPMCC) is a measure method of the linear relationship between X and Y. However, there are 2 limitations when using Pearson product-moment correlation coefficient. On one side, the data must be obtained from normal distribution in pairs. On the other side, the data are at least equidistant in logical range. Whereas the non-parameter Spearman rank correlation coefficient (SRCC) is used to measure the more generalized correlation relation (not necessarily linear).

Let (x, y) be a sample from two different entire populations: (X, Y) and its observation value is (x₁, y₁), (x₂, y₂), . . . , (x_n, y_n). If x_i and y_i are sorted by value individually, the new rank of x_i and y_i in the two sequential samples is recorded as R_{x,i} and R_{y,i} (0 ≤ i ≤ n). So, n pairs of rank numbers, (R_{x,1}, R_{y,1}), (R_{x,2}, R_{y,2}), . . . , (R_{x,n}, R_{y,n}) is obtained from 1 to n. Generally, the Spearman rank correlation coefficient formula can be recorded as follows [37]:

$$r_s = \frac{\sum_{i=1}^n (R_{x,i} - \bar{R}_x)(R_{y,i} - \bar{R}_y)}{\sqrt{\sum_{i=1}^n (R_{x,i} - \bar{R}_x)^2 \sum_{i=1}^n (R_{y,i} - \bar{R}_y)^2}} \tag{8}$$

$$\bar{R}_x = \frac{1}{n} \sum_{i=1}^n R_{x,i} \tag{9}$$

$$\bar{R}_y = \frac{1}{n} \sum_{i=1}^n R_{y,i} \tag{10}$$

If there is no same data in the X, Y sequence, then the mean value can be recorded as:

$$\bar{R}_x = \bar{R}_y = \frac{n + 1}{2} \tag{11}$$

So the formula of r_s can be further simplified to:

$$r_s = 1 - \frac{6 \sum_{i=1}^n (R_{x,i} - R_{y,i})^2}{n(n^2 - 1)} \tag{12}$$

r_s > 0 represents positive correlation and r_s < 0 represents negative correlation. |r_s| is more close to 1, the correlation between the samples is higher. Whereas |r_s| is closer to 0, the correlation between the samples is lower. Sometimes the sample with very high correlation coefficient may also come from the uncorrelated population. In order to exclude such situation, a significance test of the correlation coefficient is needed. The Student's t test provides the excellent ability to test the significance of r_s. The test formula of student's t is as follows [38]:

$$t = r_s \sqrt{\frac{n - 2}{1 - r_s^2}} \sim t(n - 2). \tag{13}$$

The general step of the significance test for the correlation coefficient is to establish the null hypothesis that H0: X and Y are related, and the alternative hypothesis that H1: X and Y is not related. Then give the confidence level α. Based on α, find out the corresponding critical value. At the end make a comparison: if |t| ≥ t^α, it is assumed that H0 is tenable and if |t| < t^α, it is assumed that H1 is tenable.

Table 3 shows the SRCC matrix of free radicals mole fraction and maximum reaction rate of NO_x. Figure 8a shows that there is a close relation between the maximum production rate of NO and the mole fraction of O, OH, H₂ (coefficient of SRCC, OH > O > H₂). Figure 8b shows that there is a close relation between the maximum production rate of N₂O and the mole fraction of O, OH, HO₂, H₂ (coefficient of SRCC, O > H₂ > OH > HO₂). Figure 8c shows that there is a close relation between the maximum production rate of NO₂ and the mole fraction of O, OH, HO₂, H₂, H₂O₂ (coefficient of SRCC, OH > H₂ > O > H₂O₂ > HO₂). All results above meet a confidence level of at least 95%. Therefore, it can be considered that the above conclusions are statistically significant and correct. At the same time, it also notes that the mole content of O, OH and H₂ has a very obvious common effect on the generation of nitrogen oxides (NO, N₂O and NO₂).

Table 3. SRCC matrix of free radicals mole fraction and maximum reaction rate of NO_x.

	X	H	O	OH	HO ₂	H ₂	H ₂ O ₂
Y	NO	0.0075	0.8586	0.8917	0.0316	0.7789	0.3368
	N ₂ O	0.1474	0.9940	0.8602	0.7699	0.9383	0.0857
	NO ₂	0.0887	0.9128	0.9789	−0.5744	−0.9639	−0.6662

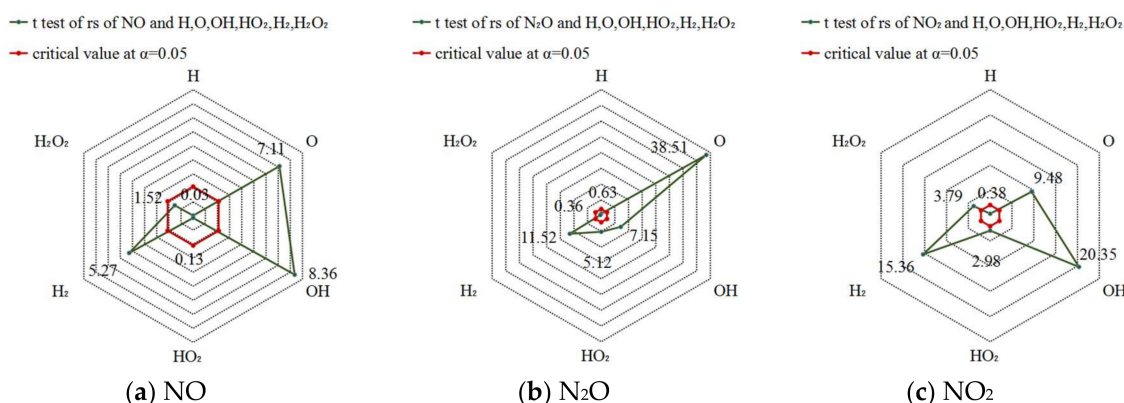


Figure 8. Result of Student’s t significance test for SRCC (confidence level $\alpha = 0.05$).

3.3.2. Sensitivity Analysis

In many research fields, sensitivity analysis is applied, and the reaction rate of components *i* is derived from mass action law:

$$\frac{dC}{dt} = f(C; K) \tag{14}$$

$$C(0) = C_0 \tag{15}$$

$$\beta_{ij}(t) = \frac{\partial C_i(t)}{\partial K_j} \tag{16}$$

The higher the sensitivity, the more important the elementary reaction *j* to the component *i*. The specific sensitivity results are shown in Figure 9, corresponding to the starting point of the second stage reaction.

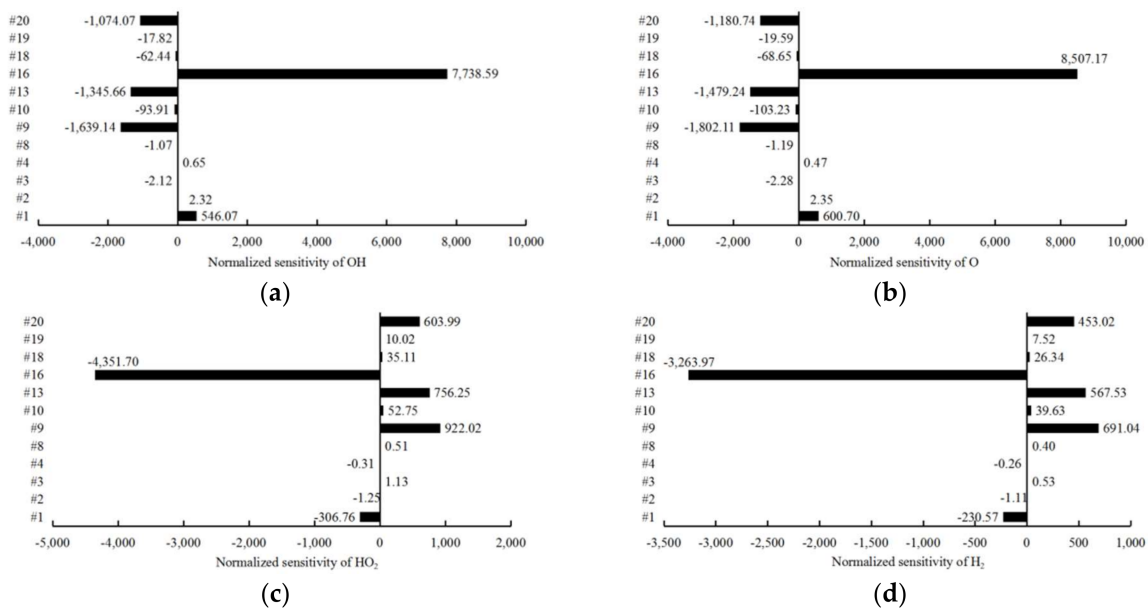


Figure 9. Sensitivity diagram of OH, O, HO₂, H₂ (at the time of the second stage starting point). (a) Normalized sensitivity of OH (b) Normalized sensitivity of O; (c) Normalized sensitivity of HO₂ (d) Normalized sensitivity of H₂.

The positive sensitivity coefficient indicates that the elementary reaction affects the generation of free radicals, and the negative sensitivity coefficient indicates that the elementary reaction affects the consumption of free radicals. The mutual influence increases with the absolute value of the sensitivity coefficient increases. From Figure 9, it is found that elementary reaction #1, #9, #13, #16 and #20 can promote or inhibit the generation of free radicals OH, O, HO₂ and H₂ than others, but the elementary reaction #16 is more important. At the same time, OH and O show a consistent sensitivity to different elementary reactions. HO₂ and H₂ show a consistent sensitivity to different elementary reactions. Whereas the sensitivity of OH, O and the sensitivity of HO₂, H₂ are antagonistic.

4. Conclusions

In this paper, a numerical investigation of the action mechanism of H, O, OH, HO₂, H₂ and H₂O₂ on the generation of nitrogen oxides with different air/fuel ratio and different WOMR was completed. The main conclusions are summarized as follows:

- An obvious result of two stages reaction processes is obtained by the numerical method. When the temperature reaches to 1000 K, the temperature rises sharply, and the mixture enters the high temperature oxidation stage. The rapid consumption of H₂O₂ and the rapid generation of OH indicates the generation of the flame surface.
- With the increase of water mass fraction, the response of the reaction of free radicals (H, O, OH, HO₂, H₂, H₂O₂) is lagged behind, meanwhile the peak value of the reaction rate decreases due to the increase of heat needed for activation reaction at the same activation energy and reaction temperature. When the water content increases 10%, the maximum generation rate of NO, N₂O, NO₂ decreases by 15.24%, 9.21%, 14.78% on average, respectively.
- According to the correlation results, maximum production rate of NO and the mole fraction of O, OH, H₂ have significant correlation relation; maximum production rate of N₂O and the mole fraction of O, OH, HO₂, H₂ have significant correlation relation; maximum production rate of NO₂ and the mole fraction of O, OH, HO₂, H₂, H₂O₂ have significant correlation relation. In contrast, OH, O and H₂ play a more significant role in the common influence of the generation of nitrogen oxides.

- According to the sensitivity results, elementary reactions #1 and #16 promote the generation of OH and O at the beginning of the second stage, but elementary reaction #9, #13 and #20 have a negative effect. Meanwhile the result is just opposite for effect of HO₂ and H₂.

Supplementary Materials: The supplementary material contains the mechanism document used in this article. The following are available online at <http://www.mdpi.com/2076-3417/8/4/490/s1>, mech.txt: it records the chemical reaction mechanism; thermo.txt: it records the thermodynamic parameters of the species; transport.txt: it records the transport parameters of the species.

Acknowledgments: This work is supported by the National Natural Science Foundation of China (NSFC, 51276079) and the Project 2017042 supported by the Graduate Innovation Fund of Jilin University. The authors appreciate the insightful comments and suggestions from the reviewers and the editor.

Author Contributions: Fengshuo He and Xiumin Yu conceived, designed and performed the experiments; Yaodong Du analyzed the data; Fengshuo He and Zezhou Guo wrote the paper.

Conflicts of Interest: The authors declare no conflict of interest.

Nomenclature

H	hydrogen atom
O	oxygen atom
OH	hydroxyl radical
HO ₂	hydroperoxyl radical
H ₂	hydrogen
H ₂ O ₂	hydrogen peroxide
M	third body
NO _x	nitrogen oxides
NO	nitric oxide
NO ₂	nitrogen dioxide
N ₂ O	nitrous oxide
EGR	exhaust gas recirculation
PM	particle matter
CO	carbon monoxide
CO ₂	carbon dioxide
HC	hydrocarbon
CA	crank angle
PLIF	planar-laser-induced fluorescence
LIF	laser-induced fluorescence
LLNL	Lawrence Livermore National Laboratory
RCM	rapid compression machine
GRI	The Gas Research Institute
C ₆ H ₅ CH ₃	methylbenzene
iC ₅ H ₁₂	isopentane
iC ₈ H ₁₈	isooctane
nC ₅ H ₁₂	n-pentane
nC ₇ H ₁₆	n-heptane
O ₂	oxygen
N ₂	nitrogen
Ar	argon
λ	excess air coefficient
WOMR	water-oil mass ratio
PPMCC	Pearson product-moment correlation coefficient
SRCC	Spearman rank correlation coefficient

Symbols

C_{pk}^0	specific heat capacity at constant pressure
H_k^0	enthalpy
S_k^0	entropy
C_{vk}^0	the specific heat capacity at constant volume
U_k^0	internal energy
G_k^0	Gibbs free energy
$a_{1k} \sim a_{7k}$	constant column
r	water-oil mass ratio
m_{water}	mass of water
m_{oil}	mass of oil
(X, Y)	two dimension random variables
(x, y)	sample of (X, Y)
$(R_{x,n}, R_{y,n})$	rank of (x_n, y_n)
$\overline{R_x}$	the mean value of R_x
$\overline{R_y}$	the mean value of R_y
r_s	Spearman rank correlation coefficient
t	index of the significance test
α	confidence level
C	n-dimensional vector of the concentration
K	the parameter of the system, which is related to the chemical reaction rate, the activation energy and so on
β_{ij}	the sensitivity of the component i to the reaction rate of the elementary reaction j

References

- Subramanian, K.A. A comparison of water–diesel emulsion and timed injection of water into the intake manifold of a diesel engine for simultaneous control of NO and smoke emissions. *Energy Convers. Manag.* **2011**, *52*, 849–857. [[CrossRef](#)]
- Awad, O.I.; Mamat, R.; Ibrahim, T.K.; Ali, O.M.; Kadirgama, K.; Leman, A.M. Performance and combustion characteristics of an SI engine fueled with fusel oil-gasoline at different water content. *Appl. Thermal Eng.* **2017**, *123*, 1374–1385. [[CrossRef](#)]
- Elsanusi, O.A.; Roy, M.M.; Sidhu, M.S. Experimental Investigation on a Diesel Engine Fueled by Diesel-Biodiesel Blends and their Emulsions at Various Engine Operating Conditions. *Appl. Energy* **2017**, *203*, 582–593. [[CrossRef](#)]
- Tauzia, X.; Maiboom, A.; Shah, S.R. Experimental study of inlet manifold water injection on combustion and emissions of an automotive direct injection Diesel engine. *Energy* **2010**, *35*, 3628–3639. [[CrossRef](#)]
- Kökkülünk, G.; Gonca, G.; Ayhan, V.; Cesur, İ.; Parlak, A. Theoretical and experimental investigation of diesel engine with steam injection system on performance and emission parameters. *Appl. Thermal Eng.* **2013**, *54*, 161–170. [[CrossRef](#)]
- Tesfa, B.; Mishra, R.; Gu, F.; Ball, A.D. Water injection effects on the performance and emission characteristics of a CI engine operating with biodiesel. *Renew. Energy* **2012**, *37*, 333–344. [[CrossRef](#)]
- Prasad, S.; Gonsalvis, J.; Vijay, V.S. Effect of Introduction of Water into Combustion Chamber of Diesel Engines—A Review. *Energy Power* **2015**, *5*, 28–33. [[CrossRef](#)]
- Kyriakides, A.; Dimas, V.; Lymperopoulou, E.; Karonis, D.; Lois, E. Evaluation of gasoline–ethanol–water ternary mixtures used as a fuel for an Otto engine. *Fuel* **2013**, *108*, 208–215. [[CrossRef](#)]
- Ge, J.; Yoon, S.; Choi, N. Using Canola Oil Biodiesel as an Alternative Fuel in Diesel Engines: A Review. *Appl. Sci.* **2017**, *7*, 881. [[CrossRef](#)]
- Ge, J.C.; Kim, H.Y.; Yoon, S.K.; Choi, N.J. Reducing volatile organic compound emissions from diesel engines using canola oil biodiesel fuel and blends. *Fuel* **2018**, *218*, 266–274. [[CrossRef](#)]
- Wang, J.-K.; Li, J.-L.; Wu, M.-H.; Chen, R.-H. Reduction of Nitric Oxide Emission from a SI Engine by Water Injection at the Intake Runner. In Proceedings of the ASME 2009 International Mechanical Engineering Congress and Exposition, Lake Buena Vista, FL, USA, 13–19 November 2009; pp. 335–340.

12. Taghavifar, H.; Anvari, S.; Parvishi, A. Benchmarking of water injection in a hydrogen-fueled diesel engine to reduce emissions. *Int. J. Hydrog. Energy* **2017**, *42*, 11962–11975. [CrossRef]
13. Lee, D.; Lee, J.S.; Kim, H.Y.; Chun, C.K.; James, S.C.; Yoon, S.S. Experimental Study on the Combustion and NO_x Emission Characteristics of DME/LPG Blended Fuel Using Counterflow Burner. *Combust. Sci. Technol.* **2012**, *184*, 97–113. [CrossRef]
14. Schulz, C.; Sick, V. Tracer-LIF diagnostics: Quantitative measurement of fuel concentration, temperature and fuel/air ratio in practical combustion systems. *Prog. Energy Combust. Sci.* **2005**, *31*, 75–121. [CrossRef]
15. Bai, L.; Zhao, S.; Fu, Y.; Cheng, Y. Experimental study of mass transfer in water/ionic liquid microdroplet systems using micro-LIF technique. *Chem. Eng. J.* **2016**, *298*, 281–290. [CrossRef]
16. Davis, S.G.; Joshi, A.V.; Wang, H.; Egolfopoulos, F. An optimized kinetic model of H₂/CO combustion. *Proc. Combust. Inst.* **2005**, *30*, 1283–1292. [CrossRef]
17. Donato, N.; Petersen, E. Simplified correlation models for CO/H₂ chemical reaction times. *Int. J. Hydrogen Energy* **2008**, *33*, 7565–7579. [CrossRef]
18. *CHEMKIN Tutorials Manual*; CHEMKIN-PRO 15131; CHEMKIN Software: San Diego, CA, USA, 2013.
19. Gordon, S.; McBride, B.J. *Computer Program for Calculation of Complex Chemical Equilibrium Compositions, Rocket Performance, Incident and Reflected Shocks and Chapman-Jouguet Detonations*; NASA Report SP-273; NASA: Cleveland, OH, USA, 1971.
20. Chen, Y.; Wolk, B.; Mehl, M.; Cheng, W.K.; Chen, J.-Y.; Dibble, R.W. Development of a reduced chemical mechanism targeted for a 5-component gasoline surrogate: A case study on the heat release nature in a GCI engine. *Combust. Flame* **2017**, *178*, 268–276. [CrossRef]
21. Mehl, M.; Pitz, W.J.; Westbrook, C.K.; Curran, H.J. Kinetic modeling of gasoline surrogate components and mixtures under engine conditions. *Proc. Combust. Inst.* **2011**, *33*, 193–200. [CrossRef]
22. Dong, S.; Yang, C.; Ou, B.; Lu, H.; Cheng, X. Experimental investigation on the effects of nozzle-hole number on combustion and emission characteristics of ethanol/diesel dual-fuel engine. *Fuel* **2018**, *217*, 1–10. [CrossRef]
23. Fu, X.-Q.; He, B.-Q.; Li, H.-T.; Chen, T.; Xu, S.-P.; Zhao, H. Effect of direct injection dimethyl ether on the micro-flame ignited (MFI) hybrid combustion and emission characteristics of a 4-stroke gasoline engine. *Fuel Process. Technol.* **2017**, *167*, 555–562. [CrossRef]
24. Zhen, X.; Wang, Y.; Liu, D. An overview of the chemical reaction mechanisms for gasoline surrogate fuels. *Appl. Thermal Eng.* **2017**, *124*, 1257–1268. [CrossRef]
25. Smith, G.P.; Golden, D.M.; Frenklach, M.; Moriarty, N.W.; Eiteneer, B.; Goldenberg, M.; Bowman, C.T.; Hanson, R.K.; Song, S.; Gardiner, W.C., Jr.; et al. GRI-Mech 3.0. Available online: http://www.me.berkeley.edu/gri_mech/ (accessed on 22 March 2018).
26. Biagioli, F.; Güthe, F. Effect of pressure and fuel–air unmixedness on NO_x emissions from industrial gas turbine burners. *Combust. Flame* **2007**, *151*, 274–288. [CrossRef]
27. Sangl, J.; Mayer, C.; Sattelmayer, T. Prediction of the NO_x-Emissions of a Swirl Burner in Partially and Fully Premixed Mode on the Basis of Water Channel LIF and PIV Measurements. In Proceedings of the ASME Turbo Expo 2013: Turbine Technical Conference and Exposition, San Antonio, TX, USA, 3–7 June 2013; p. V01BT04A058.
28. Sundaram, B.; Klimenko, A.Y.; Cleary, M.J.; Maas, U. Prediction of NO_x in premixed high-pressure lean methane flames with a MMC-partially stirred reactor. *Proc. Combust. Inst.* **2015**, *35*, 1517–1525. [CrossRef]
29. *Standard Test Method for Dynamic Viscosity and Density of Liquids by Stabinger Viscometer (and the Calculation of Kinematic Viscosity)*; ASTM D7042-16e3; ASTM International: West Conshohocken, PA, USA, 2016.
30. *Standard Test Method for Determination of Individual Components in Spark Ignition Engine Fuels by 50-Metre Capillary High Resolution Gas Chromatography*; ASTM D6733-01(2016); ASTM International: West Conshohocken, PA, USA, 2016.
31. *Standard Test Method for Research Octane Number of Spark-Ignition Engine Fuel*; ASTM D2699-17; ASTM International: West Conshohocken, PA, USA, 2017.
32. *Standard Test Method for Motor Octane Number of Spark-Ignition Engine Fuel*; ASTM D2700-17a; ASTM International: West Conshohocken, PA, USA, 2017.
33. Slack, M.W. Rate coefficient for H + O₂ + M = HO₂ + M evaluated from shock tube measurements of induction times. *Combust. Flame* **1977**, *28*, 241–249. [CrossRef]

34. Das, L. Hydrogen engine: Research and development (R&D) programmes in Indian Institute of Technology (IIT), Delhi. *Int. J. Hydrogen Energy* **2002**, *27*, 953–965. [[CrossRef](#)]
35. Verhelst, S.; Sierens, R.; Verstraeten, S. *A Critical Review of Experimental Research on Hydrogen Fueled SI Engines*; SAE Technical Paper 2006-01-0430; SAE: Warrendale, PA, USA, 2006.
36. Maghbouli, A.; Yang, W.; An, H.; Shafee, S.; Li, J.; Mohammadi, S. Modeling knocking combustion in hydrogen assisted compression ignition diesel engines. *Energy* **2014**, *76*, 768–779. [[CrossRef](#)]
37. Myers, J.L.; Well, A. *Research Design and Statistical Analysis*, 2nd ed.; Lawrence Erlbaum Associates: Mahwah, NJ, USA, 2003; ISBN 978-0-8058-4037-7.
38. Zar, J.H. Significance Testing of the Spearman Rank Correlation Coefficient. *J. Am. Stat. Assoc.* **1972**, *67*, 578. [[CrossRef](#)]



© 2018 by the authors. Licensee MDPI, Basel, Switzerland. This article is an open access article distributed under the terms and conditions of the Creative Commons Attribution (CC BY) license (<http://creativecommons.org/licenses/by/4.0/>).